수처리용 WO_3 기반 가시광촉매 개발 및 광촉매의 구조-효율 관계 규명

To develop WO_3/*g*-C_3N_4 (WCN) for water treatment by investigating structure-photocatalytic efficiency relationships

한치헌

23.04.26

수질오염의 공학적 해결

Department of Civil & Environmental Engineering, Seoul National University

Contents

Background (1/5)

❖ AOPs (Advanced Oxidation Processes)

Advanced Oxidation Process (HO· based)

UV-Photolysis
- UVC + H_2O_2
- UV + O_3
- UVA + TiO_2

Electrolysis
- SnO_2-doped
- PbO_2-doped
- TiO_2

Fenton
- H_2O_2 + Fe(II)
- H_2O_2 + Fe(II) + UV

Ultrasonic

Ozonation
- O_3
- O_3 + H_2O_2

Tetracycline

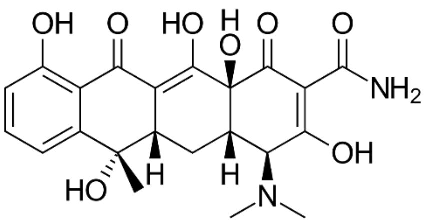

[TC]$_0$ = 100 mg/L, [H_2O_2] = 20 mg/L

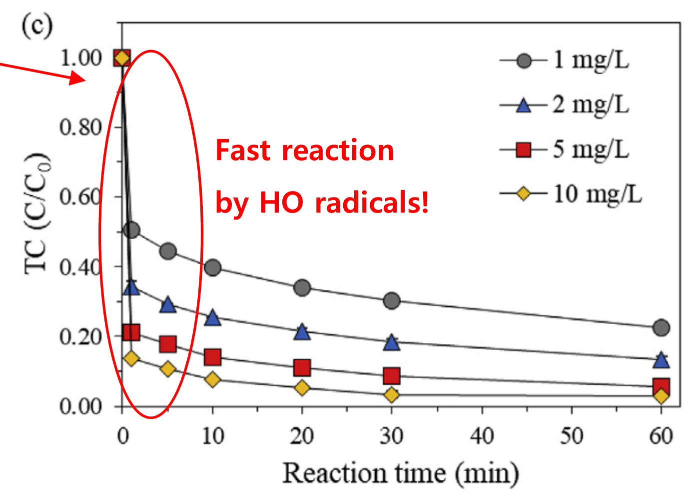

(Han *et al.*, 2020)

Background (3/5)

❖ Photocatalyst

(Fujishima *et al.*, *Nature*, 1972)

Electrochemical Photolysis of Water at a Semiconductor Electrode

ALTHOUGH the possibility of water photolysis has gated by many workers, a useful method has o developed. Because water is transparent to v cannot be decomposed directly, but only by r wavelengths shorter than 190 nm (ref. 1).

For electrochemical decomposition of water difference of more than 1.23 V is necessary electrode, at which the anodic processes occur, a where cathodic reactions take place. This poten is equivalent to the energy of radiation with a wavelength of approximately 1,000 nm. Therefore, if the energy of light is used effectively in an electrochemical system, it should be possible to decompose water with visible light. Here we

$$TiO_2 + 2\,h\nu \rightarrow 2\,e^- + 2\,p^+ \quad (1)$$
(excitation of TiO_2 by light)

$$2\,p^+ + H_2O \rightarrow \tfrac{1}{2}\,O_2 + 2\,H^+ \quad (2)$$
(at the TiO_2 electrode)

$$2\,e^- + 2\,H^+ \rightarrow H_2 \quad (3)$$
(at the platinum electrode)

The overall reaction is

$$H_2O + 2\,h\nu \rightarrow \tfrac{1}{2}\,O_2 + H_2 \quad (4)$$

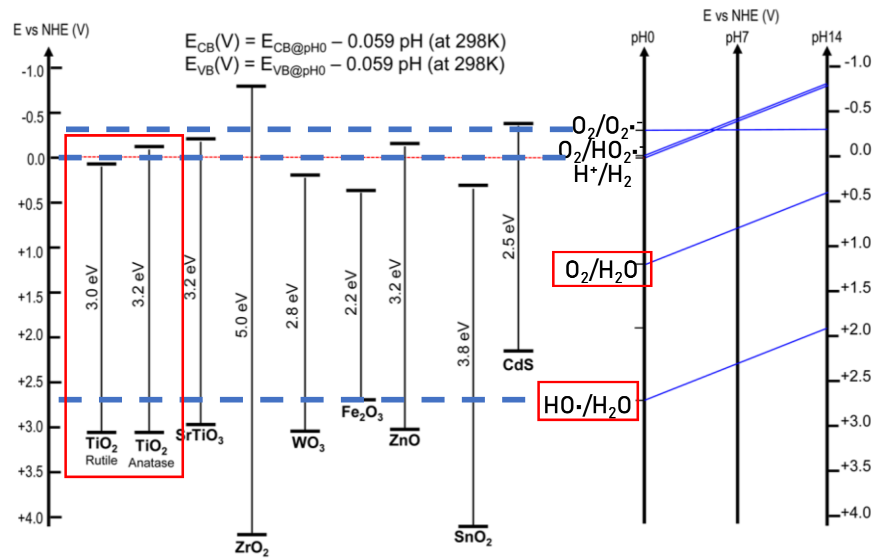

(D.D. Dionysiou *et al.*, 2016)

Background (2/5)

❖ Photocatalysis mechanism

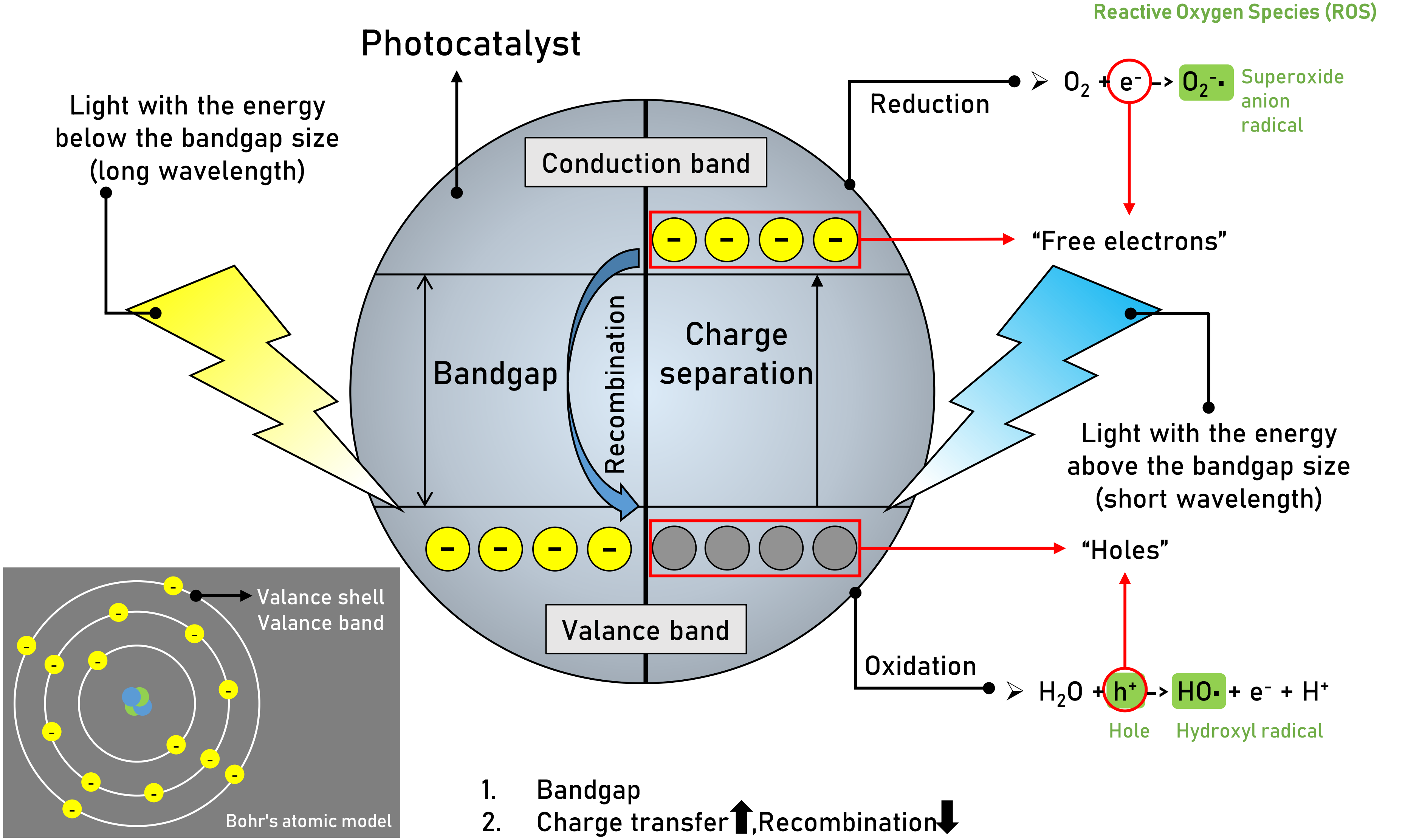

1. Bandgap
2. Charge transfer⬆,Recombination⬇

Background (4/5)

❖ UV/TiO_2 for water treatment

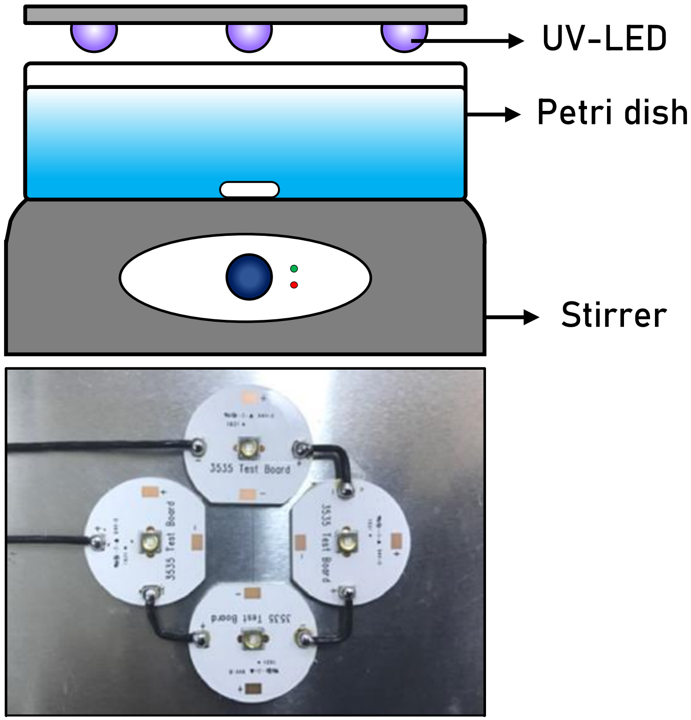

Fig. 1. Scheme of UV-LED photoreactor (up) and UV-LED module (down).

Microcystin LR (MC-LR)

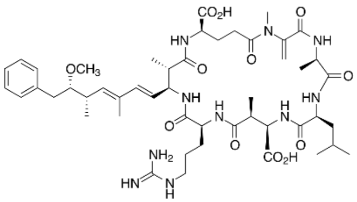

Anatoxin (ANTX)

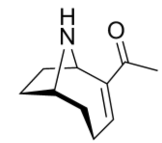

$[MC\text{-}LR]_0$, $[ANTX]_0$ = 1 mg/L, $[TiO_2]$ = 0.05 g/L

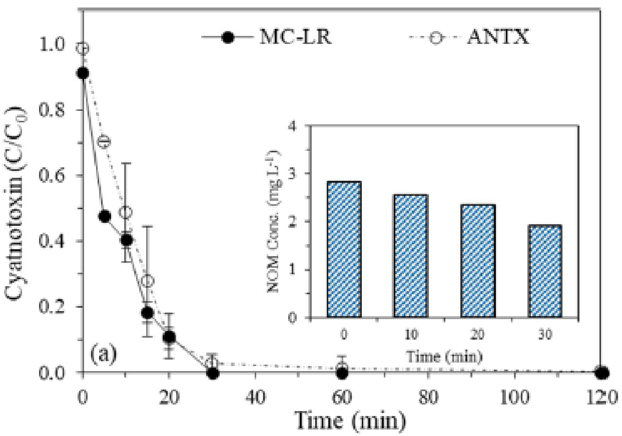

Table 1
Water quality parameters of the Han River sample.

Parameters	Value
COD (mg L^{-1})	13.0
TOC (mg L^{-1})	3.12
DOC (mg L^{-1})	2.79
pH	7.69
Conductivity (μS cm^{-1})	214.1
Turbidity (NTU)	0.16
$SUVA_{254}$ (L mg-C^{-1} m^{-1})	4.77
Alkalinity (mg L^{-1})	45

(B. Yang *et al.*, 2020)

Background (5/5)

❖ Visible light-based photocatalyst

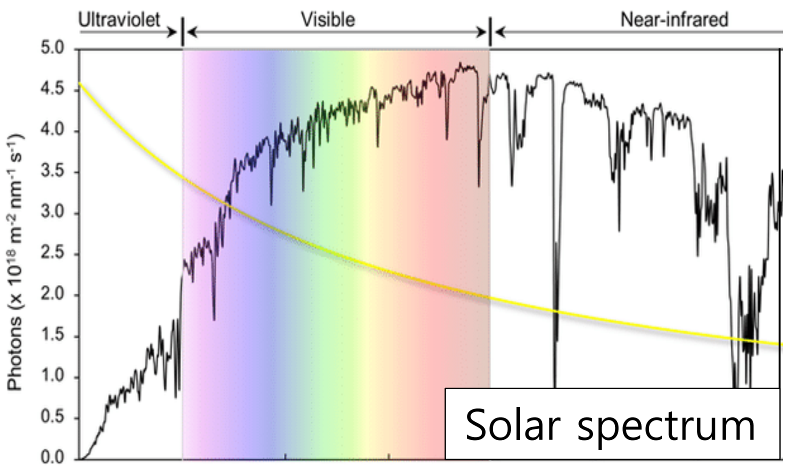

(T. Cardona *et al.*, 2018)

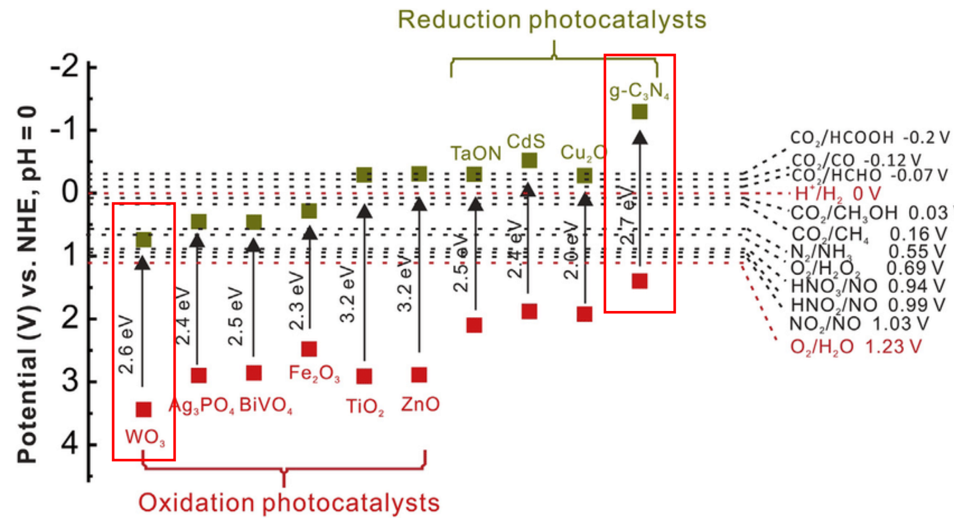

- ➢ Visible light is abundant in sunlight and has the advantage of less input energy compared to UV generation. And LED has less heat generation and power consumption, and long lifespan.
- ➢ WO_3 and *g*-C_3N_4 have band potential suitable for the use of visible light.
- ➢ Therefore, WO_3/*g*-C_3N_4 (WCN) composite is being studied as an eco-friendly visible photocatalyst for water treatment.

Literature review (1/2)

❖ Removal of organic compound using WCN under visible light irradiation

※ MB: methylene blue, Rh B: Rhodamine B, CPX: ciprofloxacin, OG: orange G RbX: Remazol brilliant red X-3BS

Year	Authors	Journal	Dosage (g/L)	Bandgap (eV)	WCN Synthesis Temp. (℃)	Target Compound	Initial Conc. (mg/L)	Light source	Reaction time (min)	Removal efficiency (%)	ROS
2014	S. Chen et al.	Appl. Catal. B	2	2.7	500->520	MB	30	Xe Lamp (500 W, >400 nm)	60	87.90%	$O_2^{-\bullet}$>$HO^{\bullet}$
2017	X. Liu et al.	Appl. Surf. Sci.	0.5	2.61, 2.67	550	MB	50	Xe Lamp (300 W, >400 nm)	90	95%	$O_2^{-\bullet}$
	L. Cui et al.	Appl. Surf. Sci.		2.69	550	Rh B	5	Xe Lamp (500 W, >420 nm)	120		
2018	B. Chai et al.	Appl. Surf. Sci.	1	2.73	550	Rh B	5	Xe Lamp (300 W, >420 nm)	180	90.40%	$O_2^{-\bullet}$>h^+>$HO^{\bullet}$
	T. Xiao et al.	Appl. Catal. B		2.73, 2.64	550	CFS TC	25	Xe Lamp (300 W, >420 nm)	120	82.00%	$O_2^{-\bullet}$, $HO^{\bullet}$
2019	A.I. Navarro-Aquilar et al.	J. Photochem. Photobiol. A	1	2.66	500	CPX OG	10 20	Xe Lamp (35 W)	240	98.00%	h^+ $O_2^{-\bullet}$
	J. Chen et al.	J. Alloys Compd.	0.33	2.7	550	Rh B	10	Xe Lamp (500 W, >420 nm)	100	96%	$O_2^{-\bullet}$>$HO^{\bullet}$>h^+
	J. Singh et al.	J. Alloys Compd.	0.5	2.16	550	MB RbX	5 45	CFL lamp (65 W)	160	97.82%	$O_2^{-\bullet}$>$HO^{\bullet}$

Literature review (2/2)

❖ GCN synthesis temperature and photocatalytic efficiency

Year	Authors	Journal	Bandgap (eV)	GCN Synthesis Temp. (℃)	Photocatalytic activity	Photocatalytic efficiency	Light source
2015	I. Papailias *et al.*	Appl. Surf. Sci.	2.76-2.37	450, 550, 650	NO oxidation	CN-450 > CN-550 > CN-650	UV, visible light
2017	Z. Lu *et al.*	Chem. Eng. J.	2.76-2.5	450, 500, 550, 600	NO oxidation	CN-500 > CN-450 > CN-550 > CN-650	150 W tungsten halogen lamp (UV&vis)
2022	B. Rani *et al.*	Chemosphere	2.87-2.83	450, 550(1h), 550(2h)	MB, RhB removal	M-450 > M-550(1h) > M-550(2h)	UV (254 nm)

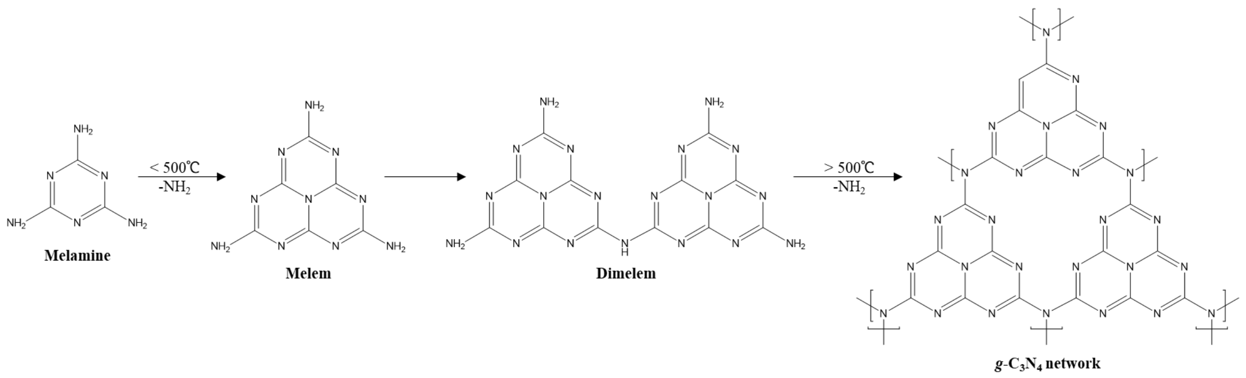

➢ There have been very few studies on the relationship between structure of WO_3/*g*-C_3N_4 and photocatalytic efficiency for removal of organic compound.

Objectives

To develop WO_3/*g*-C_3N_4 (WCN) for removing of Rhodamine B by investigating structure-photocatalytic efficiency relationships

- To characterize of WCNs for morphology, configuration and bandgap analysis photocatalyst through thermal-condensation of melamine and WO_3 at different temperatures
- To compare of photocatalytic efficiencies of WCNs by removing rhodamine B
- To investigate relationships between structure and photocatalytic efficiency of WCNs

Novelty: Investigation of relationship of the structure of WCN and photocatalytic efficiency

Photocatalytic experiment (1/2)

❖ Photoreactor

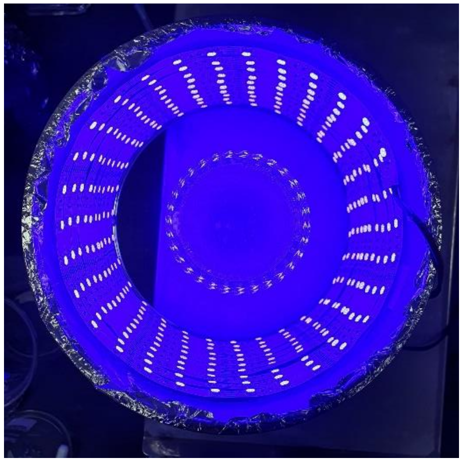

Top view of photoreactor

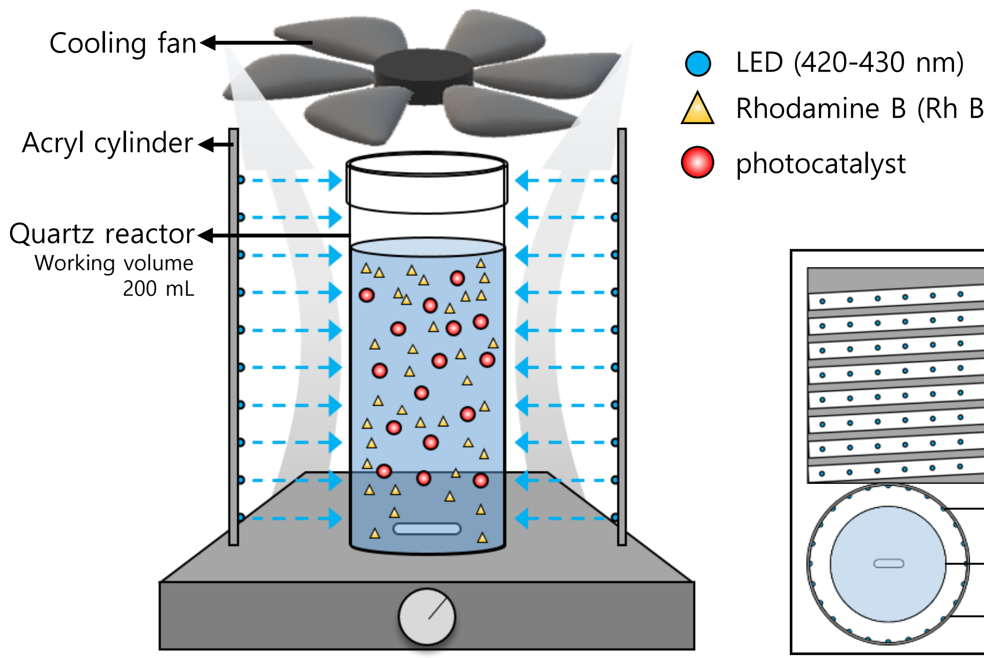

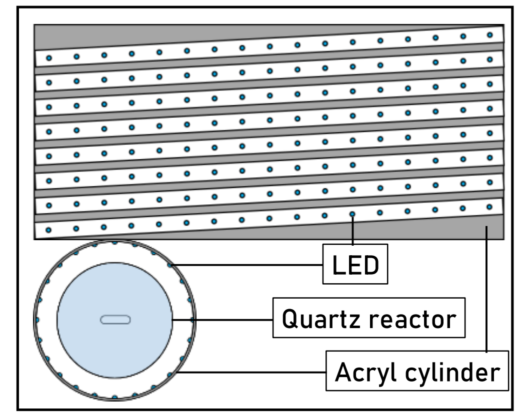

❖ Photocatalytic experiment

Ini. Conc. of Rh B: 10 mg/L, catalyst dosage: 0.5 g/L → Dark 1 hr, LED 2 hr → 1.5 mL sampling → 0.22 µm filtering → UV-vis spec. @ 553 nm

Photocatalytic experiment (2/2)

❖ Synthesis of $WO_3/g\text{-}C_3N_4$ (WCN)

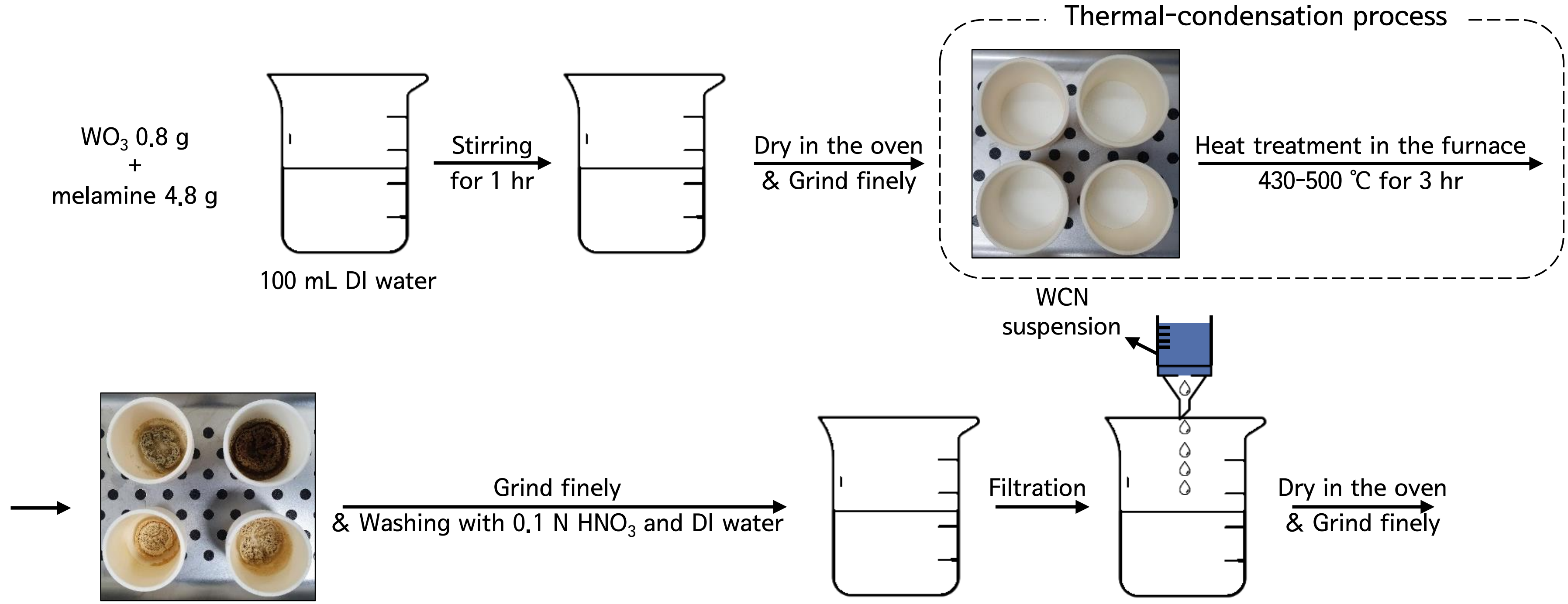

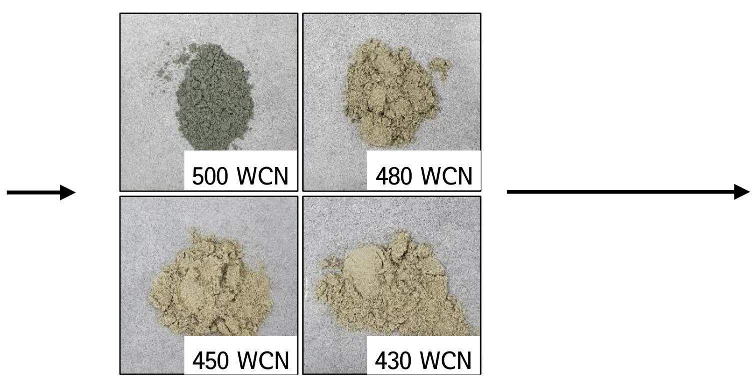

- ➢ Characterization
- ➢ Photocatalytic experiment

Material characterization

❖ SEM analysis

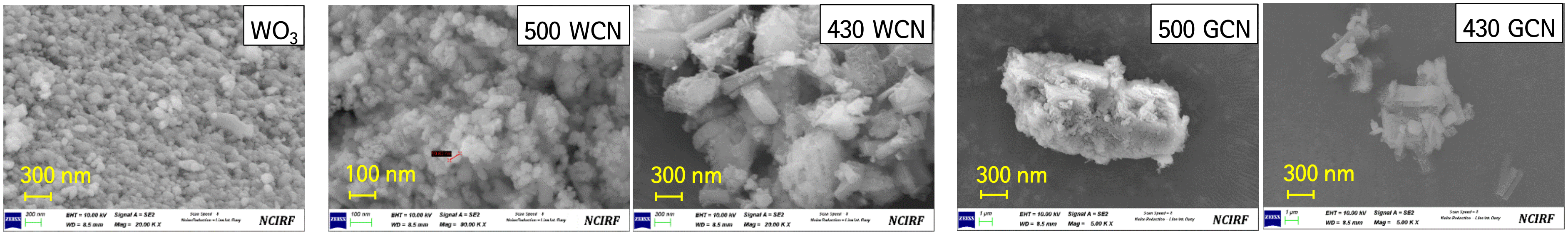

❖ TEM analysis

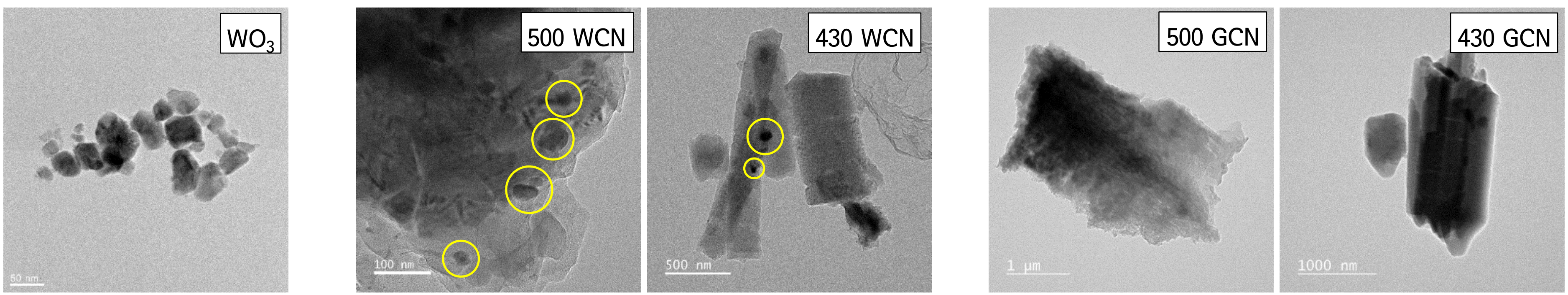

- WO_3 had a granular shape and GCN had a bulk sheet shape.
- As synthesis temperature decreased, more rod shapes were observed.
- Granular WO_3 particles were embedded in GCN.
- As in the SEM images, the rod shape was found as the synthesis temperature decreased.

Material characterization

❖ XRD analysis

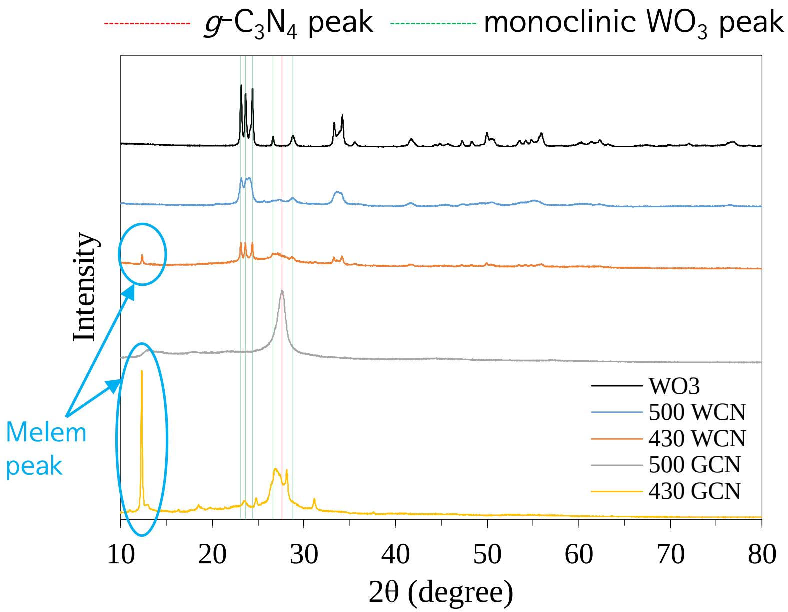

❖ FT-IR analysis

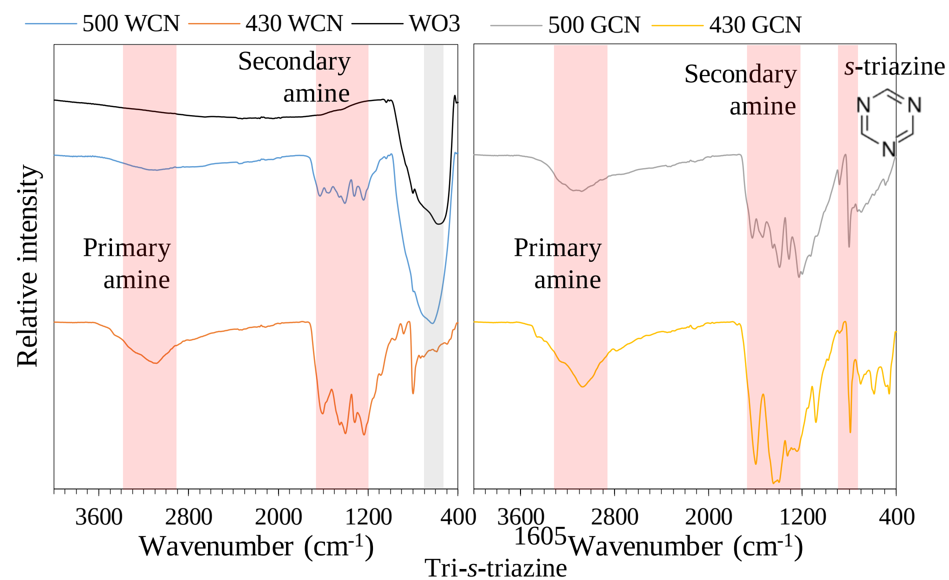

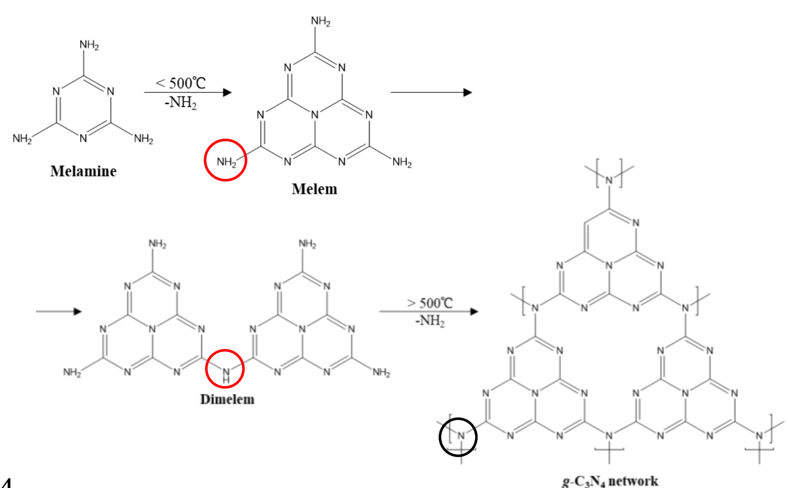

- The peak of monoclinic WO_3 was well maintained and that of melem was observed **in 430 WCN** (13.1°).
- As the treatment temperature decreased, the peak of *g*-C_3N_4 was split (27.6°), and that of melem was clearly observed (13.1°). (I. Papailias *et al.*, 2015)
- As the treatment temperature decreased, the intensity of primary (3092 cm^{-1}) and secondary amine (1400-1460 cm^{-1}) peak increased. (I. Papailias *et al.*, 2015, B. Chai *et al.*, 2018).

Photocatalytic experiment

❖ Removal of Rh B using WCNs

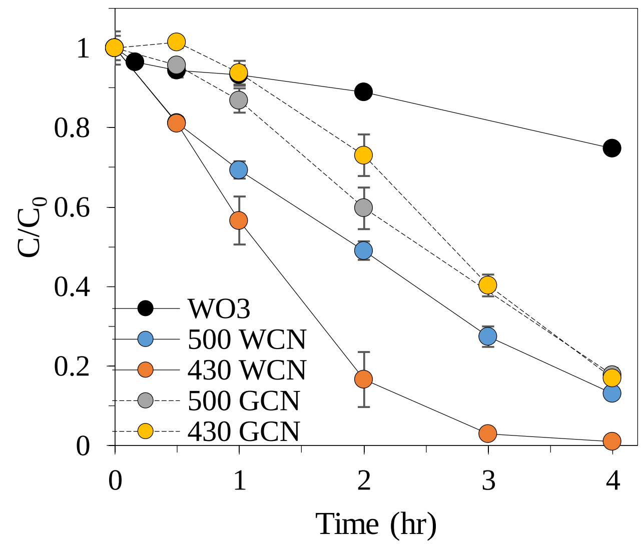

	WO_3	500 WCN	430 WCN	500 GCN	430 GCN
k (hr^{-1})	**0.1583**	**0.4057**	**1.038**	**0.3772**	**0.3309**
R^2	0.605	0.983	0.9448	0.903	0.8074

- All WCNs had better photocatalytic efficiencies than WO_3 and GCNs.
- 430 WCN showed higher photocatalytic efficiencies than 500 WCN.

Photocatalytic experiment

❖ Reactive oxygen species (ROS) scavenging test

***t*-BuOH** (HO• scavenger), **EDTA-2Na** (h^+ scavenger), **N_2 purging** (O_2 removal)

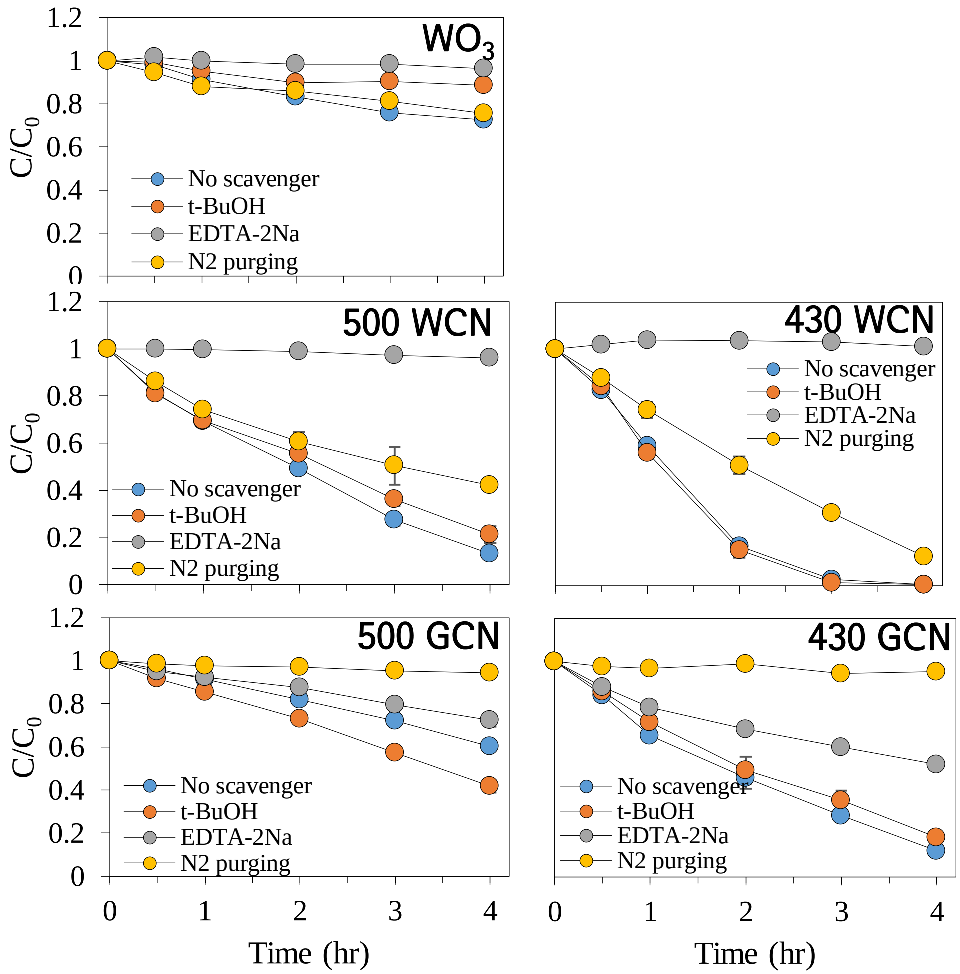

- Inhibition effect on the removal of Rh B:

  EDTA-2Na >> N_2 purging > *t*-BuOH

- Valence band hole is main ROS in vis-LED/WCN system (h^+ >> O_2-• > HO•)

Research Plans

- 500 WCN보다 430 WCN에서 condensation정도가 낮은 carbon nitride 함량이 많고, 이러한 구조의 차이가 광촉매 효율의 차이로 이어질 것으로 예상하고 있음.
  (합성온도별 WO_3와 CN의 비율을 같게 통제한 후 구조의 차이를 확인할 예정)

- TGA 및 ICP 분석을 통해 WO_3와 CN이 존재하는 비율을 비교 (500 WCN vs 430 WCN)
  비율을 같게 합성한 후 (변인 통제) WCN의 구조 및 특성들을 비교

- SS NMR을 이용한 ^{13}C, ^{15}N 분석을 통해 합성한 WCN의 구조를 더 구체적으로 파악
  430 WCN은 500 WCN에 비해 덜 condensation된 구조로 적은 수의 heptazine (3개의 CN고리)과 WO_3로 구성되어 있을 것으로 예상됨.

TGA

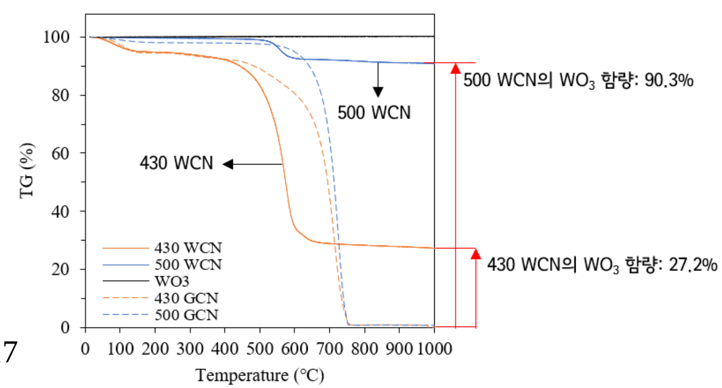

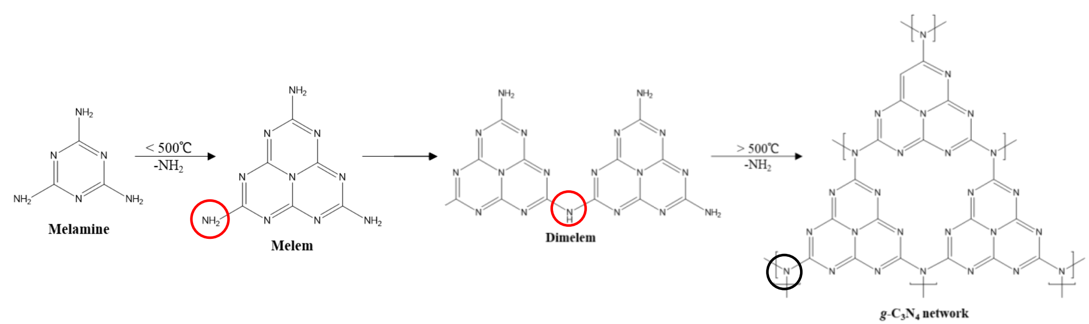

Background

❖ Pharmaceutical compounds (PhCs)

(H. Cheung *et al.*, 2019)

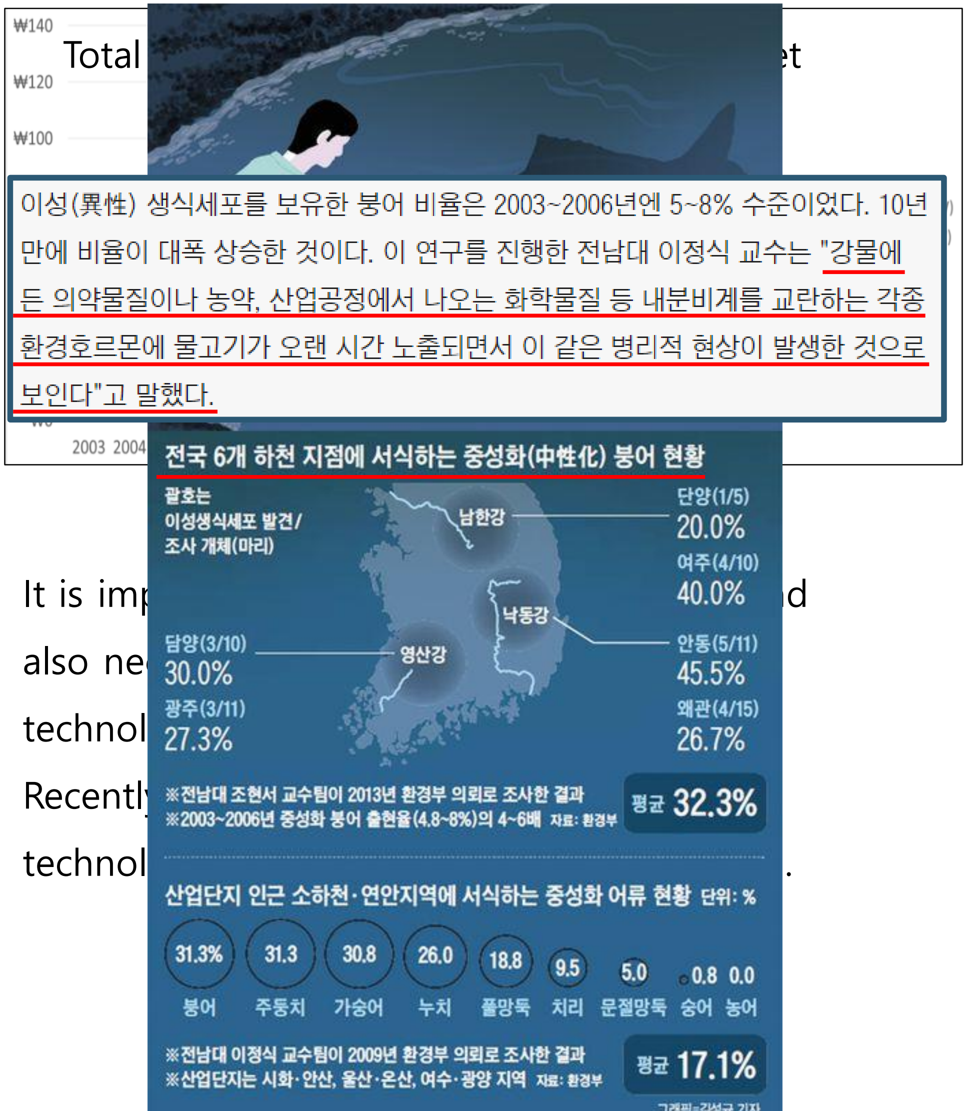

- It is imp... d also ne... technol...
- Recentl... technol... .

- The use of PhCs is steadily increasing worldwide.
- PhCs are being discharged into the water system, threatening the ecosystem and human health.

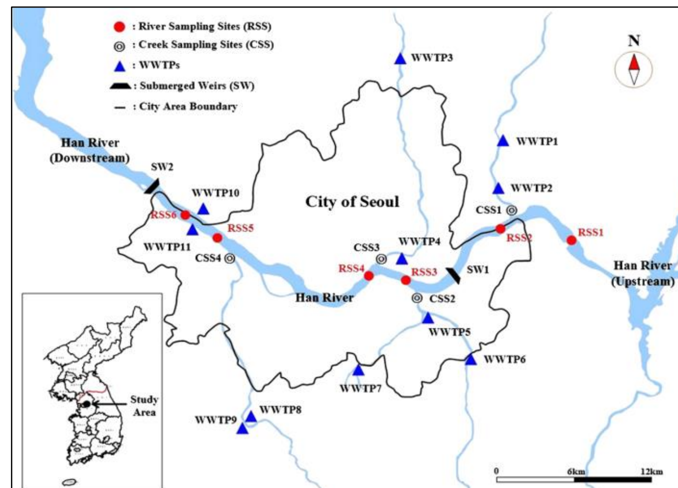

Compound	RSS mean (ng/L)	RSS max (ng/L)	RSS min (ng/L)	CSS mean (ng/L)	CSS max (ng/L)	CSS min (ng/L)
Iopromide	1013	1800	33	3745	8100	780
Atenolol	83	150	2.4	475	600	250
Naproxen	197	310	100	403	590	210
Carbamazepine	105	150	49	358	400	280
Caffeine	40	68	25	228	330	170
Ibuprofen	57	100	5.3	183	360	81
Sulfamethoxazole	56	88	15	160	190	120
Diclofenac	44	68	8.4	132	160	56

(Y. Yoon *et al.*, 2010)

14 Pharmaceutical compounds (PhCs)

negative positive

Compound	Chemical formula	MW	Structure	pKa	Compound	Chemical formula	MW	Structure	pKa
Atenolol (ATN)	고혈압 치료제 $C_{14}H_{22}N_2O_3$	266.336	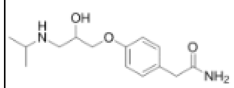	9.48/11.1	Acetylsalicylic acid (ASA)	소염진통제 $C_9H_8O_4$	180.158	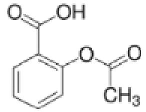	3.41
Metoprolol (MTP)	$C_{15}H_{25}NO_3$	267.364	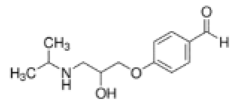	9.68	Acetaminophen (AAP)	진통제 $C_8H_9NO_2$	151.163	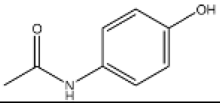	9.38
Propranolol (PPN)	$C_{16}H_{21}NO_2$	259.34	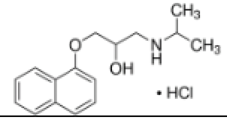	9.49	Iopromide (IPM)	조영제 $C_{18}H_{24}I_3N_3O_8$	791.112	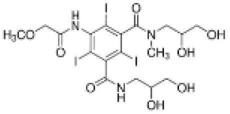	11.09
Mefenamic acid (MFA)	소염진통제 $C_{15}H_{15}NO_2$	241.28	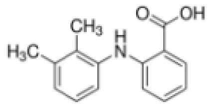	3.73	Caffeine (CAF)	신경 각성제 $C_8H_{10}N_4O_2$	194.19	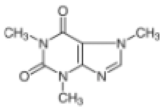	6.1/10.4
Ibuprofen (IBP)	$C_{13}H_{18}O_2$	206.29	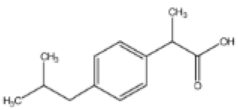	4.41	Sulfamethazine (SMZ)	항생제 $C_{12}H_{14}N_4O_2S$	278.33	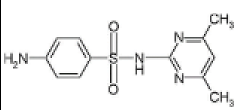	2.6/7.59
Diclofenac (DCF)	$C_{14}H_{11}Cl_2NO_2$	296.148	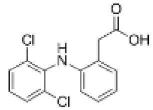	4.15	Sulfamethoxazole (SMX)	$C_{10}H_{11}N_3O_3S$	253.279	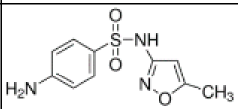	1.7/5.6
Naproxen (NPX)	$C_{14}H_{14}O_3$	230.26	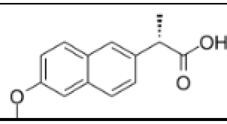	4.19	Carbamazepine (CBZ)	뇌전증 조울증 치료제 $C_{15}H_{12}N_2O$	236.269	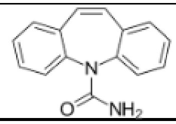	2.3/7

Analysis of 14 PhCs using LC/MS-MS

[LC/MS-MS] Agilent 1290 Infinity II / 6470 triple quadrupole

[LC column] Agilent EclipsePlus C18 RRHD 1.8 μm 2.1 × 100 mm

Positive mode					
Compound		**Precursor ion (m/z)**	**Product ion (m/z)**	**Fragmentor (V)**	**Collision energy (eV)**
Atenolol	ATN	267.2	145	161	29
Metoprolol	MTP	268.2	74.1	161	25
Propranolol	PPN	260.2	116	122	17
Caffeine	CAF	195.1	138	122	21
Carbamazepine	CBZ	237.1	194	161	21
Sulfamethazine	SMZ	279.1	186	122	17
Sulfamethoxazole	SMZ	254.1	92	122	29
Mefenamic acid	MFA	242.1	224	224	17
Acetaminophen	AAP	152.1	110	110	17
Iopromide	IPM	791.9	572.8	196	24

Negative mode					
Compound		**Precursor ion (m/z)**	**Product ion (m/z)**	**Cone voltage (V)**	**Collision energy (eV)**
Acetylsalicylic acid	ASA	137	93.1	83	17
Diclofenac	DCF	294	250	83	9
Naproxen	NPX	229.1	169	83	33
Ibuprofen	IBP	205.1	161.1	83	5

Photocatalytic experiment

❖ Photoreactor

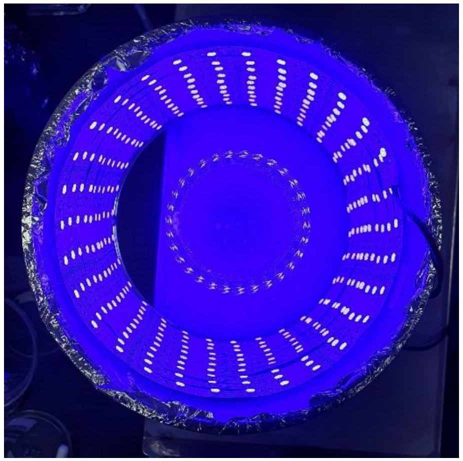

Top view of photoreactor

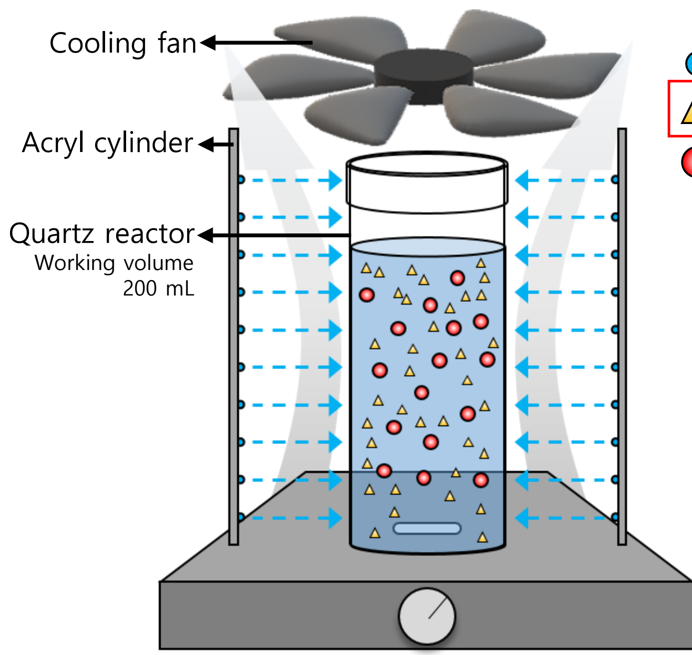

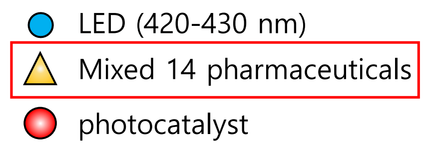

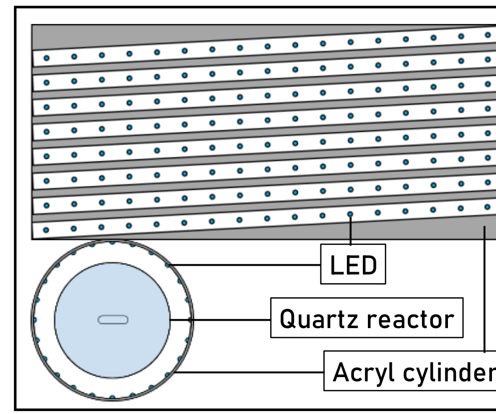

❖ Photocatalytic experiment

Ini. Conc. of PhCs: 10 μg/L
catalyst dosage: 0.5 g/L

—

Dark 1 hr
LED 2 hr

—

1 mL
sampling

—

0.22 μm
filtering

→

Analysis
Using LC/MS-MS

Photocatalytic experiment

❖ WO_3와 430 WCN의 14 PhCs 제거 효율 비교

촉매에 의한 PhCs의 흡착량에 따른 분류

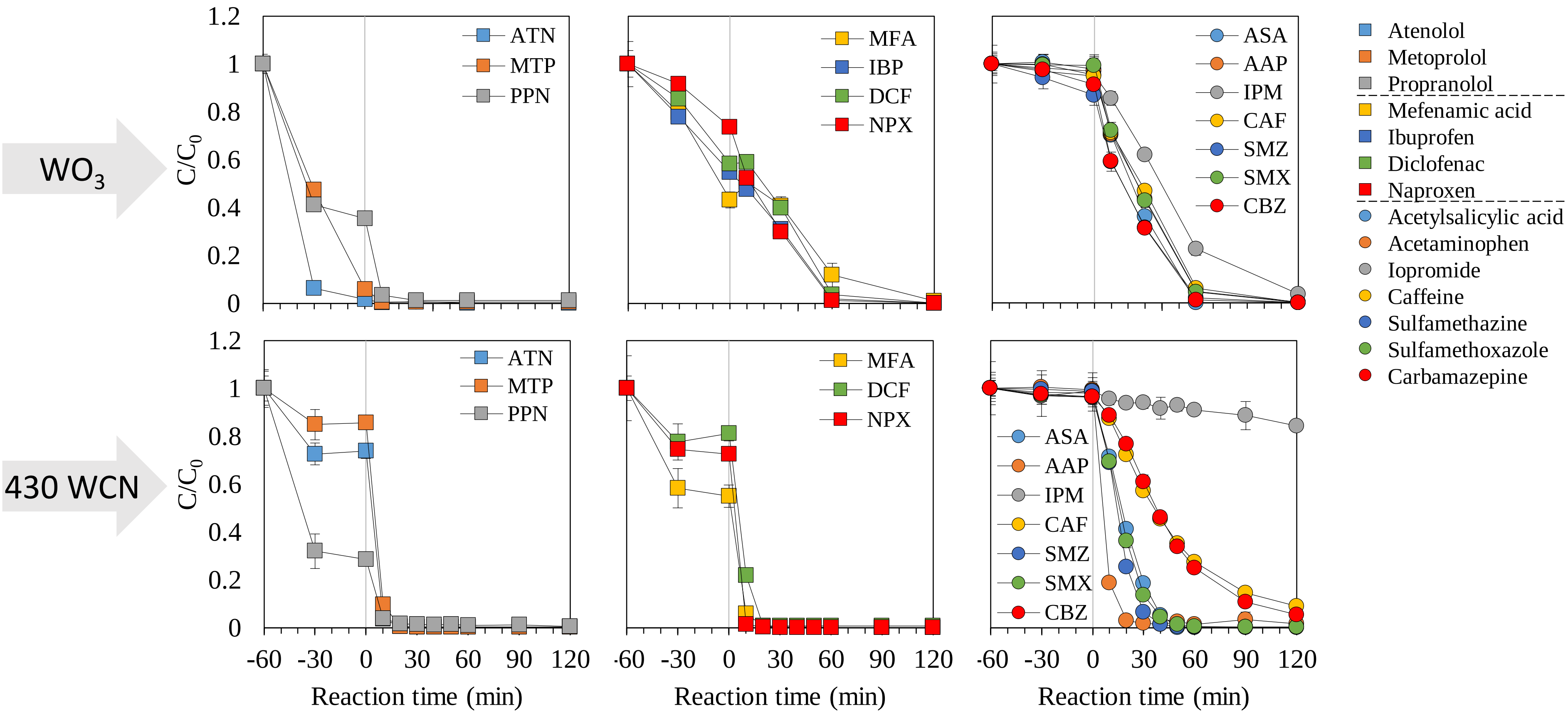

- 흡착률이 낮은 물질 중 ASA, AAP, SMZ, SMX의 광촉매에 의한 제거율은 WO_3 보다 430 WCN에서 더 높았음.
- 예상과는 다르게 CAF, CBZ는 430 WCN 에서 더딘 제거속도를 보였고, IPM의 경우 430 WCN에서 제거율이 현저히 감소하였음.
- 이는 HO· 기반인 WO_3와 h^+, O_2^{-}·기반인 430 WCN의 제거 기작 차이 때문인 것으로 보이며, 특히 IPM은 h^+, O_2^{-}· 와의 반응성이 매우 낮은 것으로 생각됨.

Summary

- WO_3 보다 개선된 WCN 가시광촉매를 합성하였고 이를 14 PhCs의 제거를 통해 확인하였음.

- HO•이 main ROS인 WO_3와 달리 WCN은 h^+가 main ROS인 것으로 확인되었고, 이러한 ROS 생성 기작 차이로 인해 14 PhCs의 제거 양상도 다르게 나타남.

- 모든 PhCs들을 효과적으로 제거하기 위해 기존보다 우수한 성능의 WCN의 개발 필요성을 확인하였음.

Thank You

Energy band potential of WO_3 photocatalyst

❖ Valence band, conduction band and bandgap energy

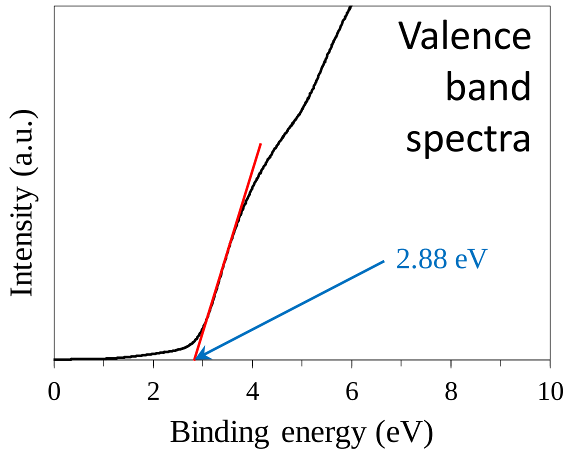

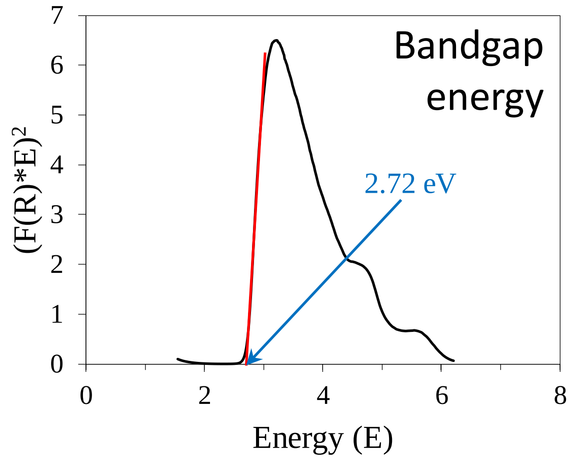

- Bandgap = VB – CB
- Bandgap energy: 2.72 eV
- VB potential: 2.88 eV
- CB potential: 0.16 eV

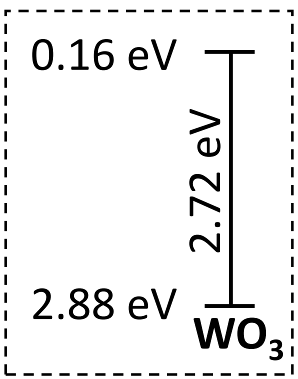

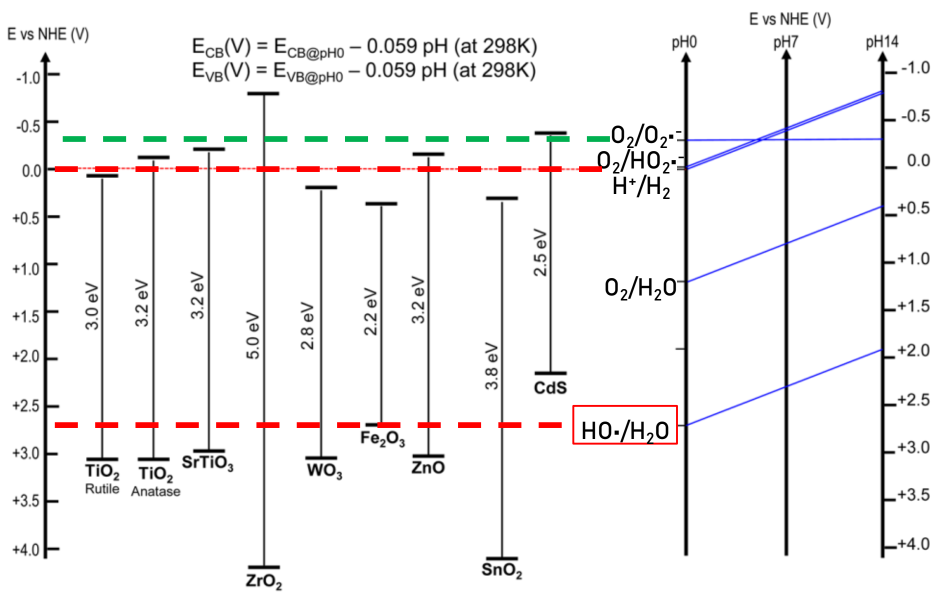

(D.D. Dionysiou et al., Photocatalysis: Applications, 2016)

➢ Valence band of WO_3 has oxidative potential to oxidize H_2O to $HO^{\bullet}$.

Bandgap energy of photocatalysts

❖ Bandgap energy analysis using UV-DRS

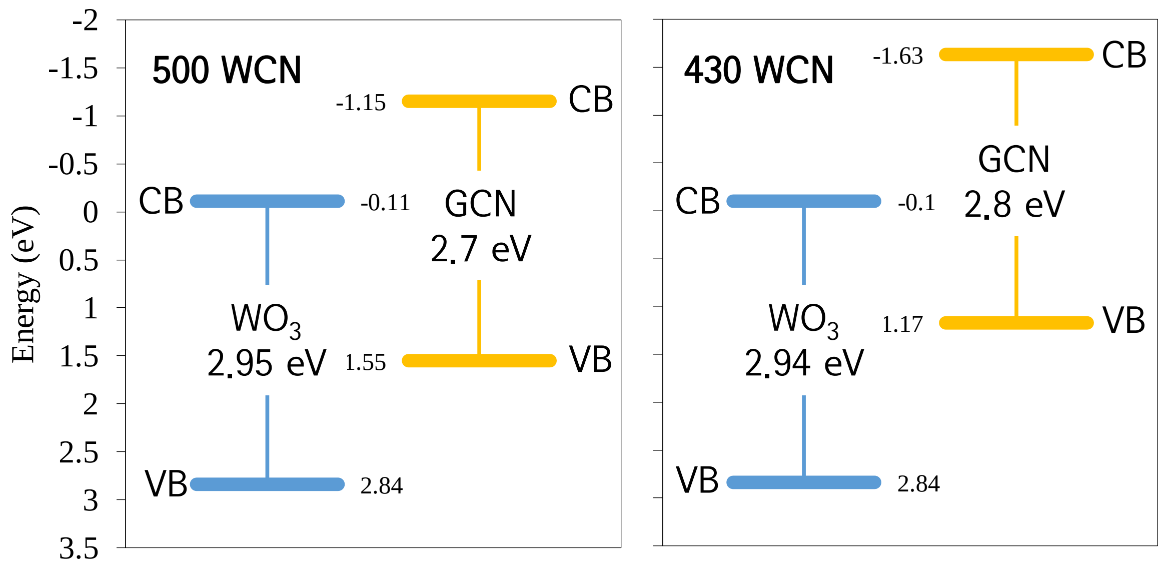

<Band structure of WCNs>

Synthesis emperature (°C)	Bandgap energy (eV)		
	WCN	WO_3	GCN
500	2.83	2.95	2.7
430	2.98	2.94	2.8

➢ As the treatment temperature decreased, the bandgap size of WCN and GCN gradually increased.

➢ However, there was no change in the bandgap size of heat-treated WO_3 photocatalysts.

Photocatalytic experiment

❖ Removal of Rh B using WCNs

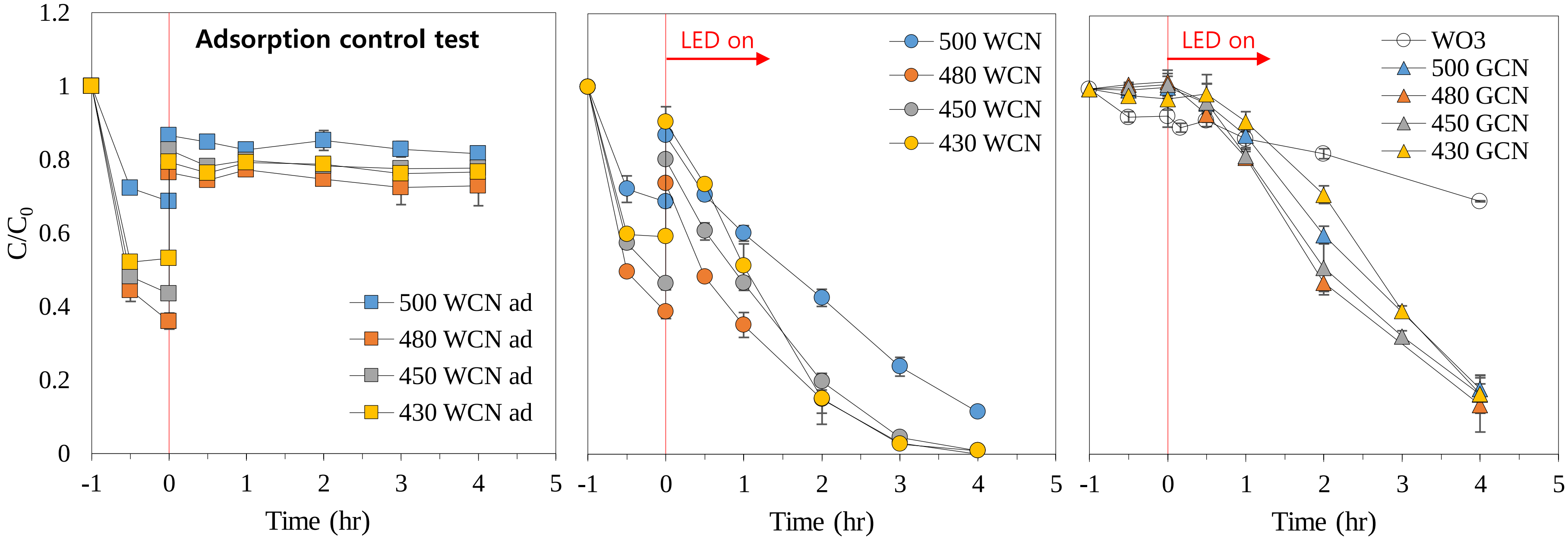

	500 WCN	480 WCN	450 WCN	430 WCN	WO_3	500 GCN	480 GCN	450 GCN	430 GCN
k (hr^{-1})	**0.4057**	**0.9704**	**0.9497**	**1.038**	**0.1583**	**0.3772**	**0.4484**	**0.4262**	**0.3309**
R^2	0.983	0.9579	0.9529	0.9448	0.605	0.903	0.9243	0.9154	0.8074

- All WCNs had better photocatalytic efficiencies than WO_3 and GCNs.
- Lower temperature WCNs (480-430 WCN) showed higher photocatalytic efficiencies than 500 WCN.